Journal of Applied Polymer Science

Synthesis, characterization, and cytotoxicity of star-shaped polyester-based elastomers as controlled release systems for proteins

Fangyuan Guo,[1] Wei Zhang,[2] Xiaohong Pei,[1] Xia Shen,[1] Qinying Yan,[1] Weiyong Hong,[3] Gensheng Yang[1]

[1]College of Pharmaceutical Science, Zhejiang University of Technology, Hangzhou 310014, China
[2]College of Mechanical Engineering, Zhejiang University of Technology, Hangzhou 310014, China
[3]Taizhou Municipal Hospital of Zhejiang Province, Taizhou 318000, China
Correspondence to: G. Yang (E-mail: yanggs@zjut.edu.cn)

ABSTRACT: With the growing number of therapeutic proteins on the market, effective delivery systems are receiving particular attention. In this study, biodegradable elastomers, intended for protein drug delivery and based on methacrylic tripoly(ε-caprolactone-*co*-D,L-lactide) cyclic ester with different ratios of ε-caprolactone to D,L-lactide and methacrylic bipoly[ε-caprolactone-*b*-poly(ethylene glycol)-*b*-ε-caprolactone], were synthesized and characterized. The degradation behavior, bovine serum albumin (BSA)-releasing kinetics, and cytotoxicity of the elastomers *in vitro* were investigated. The elastomers were degraded by the hydrolysis of the ester bond; this resulted in pH changes, which further affected the degradation rate. The BSA-releasing behavior was strongly dependent on the diffusion mechanism. In the diffusion-controlled period, nearly sustained and stable BSA release was achieved. Furthermore, the elastomers displayed good biocompatibility, as demonstrated by a 3-(4,5-dimethyl thiazol-2-yl)−2,5-diphenyl tetrazolium bromide assay and inflammation–induction experiments, and are considered promising candidates for the controllable delivery of protein drugs. © 2016 Wiley Periodicals, Inc. J. Appl. Polym. Sci. **2016**, *133*, 43393.

KEYWORDS: biomaterials; crosslinking; drug delivery systems; elastomers; proteins

Received 4 September 2015; accepted 27 December 2015
DOI: 10.1002/app.43393

INTRODUCTION

Over the past few decades, peptide and protein drugs have been greatly developed because of their high curing effectiveness in metabolic disease, tumors, and infections.[1,2] A number of protein and peptide drugs, including monoclonal antibodies and enzymes, have entered the marketplace after approval by the U.S. Food and Drug Administration and regulatory agencies in other countries. Protein drugs have become one of the most important areas of activity in modern pharmaceutical research and in the biopharmaceutical drug market. However, their short half-life and high overall clearance rate are significant problems that restrict clinical applications.[3,4]

With the development of materials science, biodegradable polymers have been widely used in the design of controlled delivery systems, tissue engineering, regenerative medicine, gene therapy, and so on, because of their distinctive biodegradability and biosecurity.[5–10] Additionally, the characteristics of encapsulation, water uptake, thermomechanical properties, biodegradation, drug-release rate, scaffold porosity, and toxicity are considered important impact factors for successful delivery.[11] Numerous delivery devices, such as nanoparticles,[12–15] microsphere,[16–18] and liposomes,[19] have been reported. They have not been easily applicable for peptide and protein drugs, which require sustainable and stable release kinetics over a prolonged period of time.[20,21]

Elastomers, synthesized by photocrosslinking and based on star-shaped polycyclic esters, as a new generation of advanced biocompatible and biodegradable materials for implantable drug-delivery devices have received extensive attention because of their unique branched structures and physicochemical and mechanical properties.[22] In contrast to conventional thermal crosslinking techniques, the light-activated curing in the preparation of biodegradable elastomers offers several advantages for peptide- and protein-delivery systems. The preparing process is easier and faster, and the activity of the protein is better retained. Therapeutically, photocured elastomers used in controlled delivery [interleukin-2,[23] interferon γ,[23,24] vascular

This article was published online on 18 Jan 2016 . An error was subsequently identified. This notice is included in the online and print versions to indicate that both have been corrected 27 Jan 2016.

endothelial growth factor,[23,25,26] vitamin B_{12},[27] and MFFD (19-mer peptide fragment of serum amyloid A with the sequence ADQAANEWGRSGKDPNHFR)[28] as model drugs] have been reported.

Generally, biodegradable elastomers synthesized from star-shaped polycyclic esters are strongly lipophilic; this makes them beneficial for drug-loading and drug-release kinetics. However, the long degradation periods resulting from their strong lipophilicity greatly hinder their applications in these delivery systems. Hence, in this study, methacrylic bipoly[ε-caprolactone-*b*-poly(ethylene glycol)-*b*-ε-caprolactone] (CLPEGCLMA) was introduced as a new hydrophilic precursor to enhance the hydrophilicity of the system. This was combined with designed methacrylic tripoly(ε-caprolactone-*co*-D,L-lactide) cyclic esters (MASCPs) having different ε-caprolactone/D,L-lactide (CL/LA) ratios. Novel elastomers based on the MASCPs and CLPEGCLMA were fabricated by UV crosslinking. The physical and thermal properties of the elastomers were determined, and the factors controlling their degradation and protein-release behaviors were studied. Furthermore, the toxicology of the elastomers was assessed to determine their potential as candidates for protein-delivery systems.

EXPERIMENTAL

Materials

D,L-Lactide (D,L-LA; 99%; Alfa Aesar, China) was recrystallized from dry toluene, and ε-caprolactone (ε-CL; 97%; Sigma Aldrich, China) was dried over CaH_2 and distilled before use. Poly(ethylene glycol) (PEG; molecular weight = 5500), stannous 2-ethyl hexanoate (95%), lipopolysaccharide (LPS), and Dulbecco's modified Eagle's medium (DMEM) were obtained from Sigma Aldrich (China). L929 and RAW264.7 cells were purchased from the cell bank of the Chinese Academy of Sciences (China). 4-Dimethyl aminopyridine (DMAP), 2,2-dimethoxy-2-phenyl acetophenone (99%), bovine serum albumin (BSA; >98%), methacrylic anhydride (94%), glycerol, fetal bovine serum, and other chemicals were obtained from Aladdin (China).

Copolymer Synthesis

Star poly(ε-caprolactone-*co*-D,L-lactide) (SCP) with different CL/LA ratios and poly[ε-caprolactone-*b*-poly(ethylene glycol)-*b*-ε-caprolactone] (CLPEGCL) were synthesized via ring-opening melt polymerization. The representative synthesis process of SCP (glycerol/ε-CL/D,L-LA molar ratio = 1:12.5:7.5) was as follows: glycerol (1 mmol), ε-CL (12.5 mmol), and D,L-LA (7.5 mmol) were transferred into a 5-mL glass ampule and then placed in an oven at 140°C for 15–20 min. After a homogeneous melt was obtained, stannous 2-ethyl hexanoate (0.1235 mmol, catalyst) was added and mixed well. Then, the ampule was sealed under dry nitrogen protection, and the polycondensation was carried out for 8 h at 140°C. After the reaction was complete, the SCP was purified twice by precipitation from methanol at −20°C for 2 h. The precipitate was then filtered and placed *in vacuo* at 40°C for 24 h. The other SCPs (with ratios of 1:10:10 and 1:7.5:12.5) were prepared in the same way.

To prepare the linear copolymer of CLPEGCL, PEG (1 mmol), ε-CL (30 mmol), and stannous 2-ethyl hexanoate (0.0926 mmol) were mixed in an ampule, which was sealed and reacted for 12 h under the same conditions as used for the foregoing SCP synthesis. Then, the product was purified twice by precipitation from a dichloromethane (DCM) solution into diethyl ether (1:15 v/v). Purified CLPEGCL was obtained by filtration and *in vacuo* drying at 40°C for 24 h.

The structures of all of the copolymers were determined by ^{1}H-NMR in $CDCl_3$ (Avance III 500 MHz, Bruker). The number-average molecular weight (M_n) values and polydispersity indices (PDIs) of the polymers were characterized by gel permeation chromatography (GPC) analysis (Waters Alliance GPC system, multiangle laser light-scattering detector) with a Phenogel linear (2) 5-μm GPC column with tetrahydrofuran as the eluent (flow rate = 1 mL/min) at 35°C.

Acrylation of the Copolymers

To introduce the UV crosslinkable end groups, the purified copolymers were acrylated with methacrylic anhydride in anhydrous DCM containing DMAP and triethylamine as the catalyst and acid scavenger, respectively. The reaction was performed under dry nitrogen at 50°C for 24 h. The purification process was the same as for each copolymer synthesis. The degree of methacrylation (DMA) was calculated by an ^{1}H-NMR spectrogram. For the acrylated copolymers (MASCPs and CLPEGCLMA), the optimized molar ratios of the copolymer (SCPs and CLPEGCL), methacrylic anhydride, DMAP, and triethylamine during preparation were 1:3:0.5:1.5 and 1.5:3:0.5:1.5, respectively.

Preparation of the Crosslinked Elastomers

The elastomers were synthesized by the photocrosslinking method. In this study, 30% CLPEGCLMA was chosen as an optimal composition on the basis of our previous study, in which we found that the elastomers became more rigid and their hydrophilicity increased as the CLPEGCLMA content increased. However, when the CLPEGCLMA content exceeded 30%, a partial disintegration phenomenon was observed; this is disadvantageous to stable and sustained drug release.

Briefly, 2,2-dimethoxy-2-phenyl acetophenone (150 mg) was dissolved in DCM (10 mL) as the photoinitiator solution. MASCP (70 mg) with different CL/LA ratios and CLPEGCLMA(30 mg) were placed in a 2-mL glass vial and then dissolved by the addition of 100 μL of the photoinitiator solution. After complete dissolution, the vial was exposed to UV irradiation for 5 min at 365 nm with an intensity of 20 mW/cm^2 to form an elastomeric cylinder about 10 mm in diameter and 3 mm in thickness. The cylinder was dried *in vacuo* at 40°C for 24 h to remove the DCM.

Elastomer Characterization

The gel content (GC), porosity volume (PV), and swelling degree (SD) of the elastomers were assessed by the gravimetric analysis method.

For GC, 100 mg of the elastomer sample was immersed in 2 mL of anhydrous DCM for 8 h to remove the residual acrylated uncrosslinked copolymers. After that, the samples were dried *in vacuo* at 40°C to a constant weight. The GC value was calculated according to eq. (1):

$$\mathrm{GC}\ (\%) = W_1/W_0 \times 100 \quad (1)$$

where W_0 is the initial weight of the dry sample and W_1 is the final (dry) weight of the sample after sol extraction.

The procedures for determining PV and SD were similar. The elastomer samples (100 mg) were immersed in 2 mL of anhydrous isopropyl alcohol and deionized water, respectively, for 2 days. The samples were retrieved and blotted to remove excess solvent on the surface, and then, the absolute weights were measured. The values of PV and SD were calculated with eqs. (2) and (3):

$$\text{PV (mL)} = (W_i - W_0)/\rho \quad (2)$$

$$\text{SD (\%)} = (W_s - W_0)/W_0 \times 100 \quad (3)$$

where W_i is the wet weight of the sample after immersion in anhydrous isopropyl alcohol, ρ is the density of isopropyl alcohol (mg/mL), and W_s is the wet weight of the sample after immersion in deionized water.

Thermal analysis was conducted with differential scanning calorimetry (Netzsch DSC 200F3). We carried out the experiments by heating the samples from room temperature to 100°C, then cooling them to −80°C, and then heating them to 100°C at a rate of 10°C/min. Each terminal point was sustained for 3 min, and the glass-transition temperatures (T_g) were measured from the second heating cycle.

The morphologies of sections of different elastomers were observed by scanning electron microscopy (SEM) on a Hitachi S-4700 instrument at 100 and 500× magnifications.

In Vitro Degradation

In vitro degradation was carried out in a 2-mL vial containing an elastomeric cylinder (100 mg in weight, 10 mm in diameter, and 3 mm in thickness) and 1 mL of sterile isotonic phosphate-buffered saline (PBS; 0.1*M*) at pH 7.4 on a shaker at 125 rpm and 37°C. Then, the PBS was replaced at different time points (1, 3, and 7 days and then once a week). For every given time point, three samples of each elastomer were removed and washed with deionized water three times, and the pH of the media was measured. The samples were later dried at 40°C *in vacuo* for 48 h. The final weight of the elastomeric cylinder was measured, and the degradation ratio was calculated as follows:

$$\text{Degradation ratio (\%)} = (W_0 - W_d)/W_0 \times 100 \quad (4)$$

where W_d is the final (dry) weight of the sample after degradation.

BSA-Loaded Device Preparation

We prepared the BSA by grinding and sieving it through a #200 Tyler sieve to ensure a particle size of less than 75 μm. Then, MASCP (70 mg), CLPEGCLMA (30 mg), and BSA (1 mg) were put into a 2-mL glass vial and mixed with the photoinitiator solution (100 μL). After it was dispersed well, the mixture was subjected to UV irradiation to form an elastomer. The detailed procedure was the same as that of the preparation of the cross-linked elastomers, as described previously.

In Vitro Release

The *in vitro* release studies were performed under the same conditions of degradation with same size cylinder sample. At predetermined time intervals (every day in the first week and twice in a week thereafter), 0.5 mL of the supernatant was collected and replaced with isopycnic fresh PBS. A total of three devices were used for each release experiment. The concentration of BSA in the release medium was measured with the bicinchoninic acid protein assay.[29]

Cytotoxicity Assays: 3-(4,5-Dimethyl thiazol-2-yl)−2,5-diphenyl Tetrazolium Bromide (MTT) and Inflammation-Induced Experiment

Mouse embryonic fibroblasts and mice macrophages (L929 and RAW264.7) were used for the MTT and inflammation–induction experiment, respectively. The cells were grown in DMEM supplemented with 10% v/v fetal bovine serum at 37°C in 5% CO_2/air and 100% relative humidity. The cells were plated in 24-well plates at a density of 1×10^5 cells/well in 1 mL of medium and allowed to attach for 24 h before the initiation of the experiments.

The photocured elastomer material was cut into approximate 20-μm slices (ca. 30 mg) and sterilized with 75% ethanol and UV irradiation. Later, the slices were immersed in 6 mL of serum-free DMEM at 37°C for 2, 4, and 7 days, respectively. The morphologies of the L929 fibroblast cells were evaluated with an inverted microscope (Diaphot, Leica). Meanwhile, for the MTT assay, cells with only medium served as negative controls. Sample of each sterile degradation medium (20 μL/well), which were collected on the 2nd, 4th, and 7th days, and the control medium were directly into six wells containing attached cells and incubated at 37°C, respectively. Later, the 20-μL MTT labeling reagent was added to each well and incubated for 4 h under a humidified atmosphere at 37°C. The unreacted dye was removed by aspiration, and the purple formazan crystals were dissolved in 150 μL of dimethyl sulfoxide by shaking for 10 min. The absorbance was measured at 570 nm with a Multiskan Spectrum instrument (Spectramax M2e). The cell viability (%) as related to the control cells cultured in medium without polymer was calculated as follows:[30]

$$\text{Cell viability (\%)} = [\text{A}]_{\text{test}}/[\text{A}]_{\text{control}} \times 100 \quad (5)$$

where $[\text{A}]_{\text{test}}$ is the absorbency of the test solution and $[\text{A}]_{\text{control}}$ is the absorbency of the negative control solution.

For the inflammation–induction experiment, RAW264.7 cells were used. Cells with LPS (10ng/mL) and cells with only medium served as positive and negative controls, respectively. An aliquot of each sterile degradation medium (20 μL/well) was collected on the 4th day, and the positive and negative control media were directed into four wells containing the attached cells and incubated at 37°C for 24 h, respectively. After incubation, the supernatant was removed, and the content of tumor necrosis factor α (TNF-α) and interleukin-1β (IL-1β) induced by the media were measured by enzyme-linked immunosorbent assay analysis.

RESULTS AND DISCUSSION

Polymer Characterization

Our goal was to prepare novel photocrosslinked elastomers based on MASCPs (lipophilic precursors) and CLPEGCLMA (hydrophilic precursor). In Figures 1 and 2, the characteristic ^{1}H-NMR spectra, complete with peak assignments, of the copolymers and their acrylated products are illustrated. As

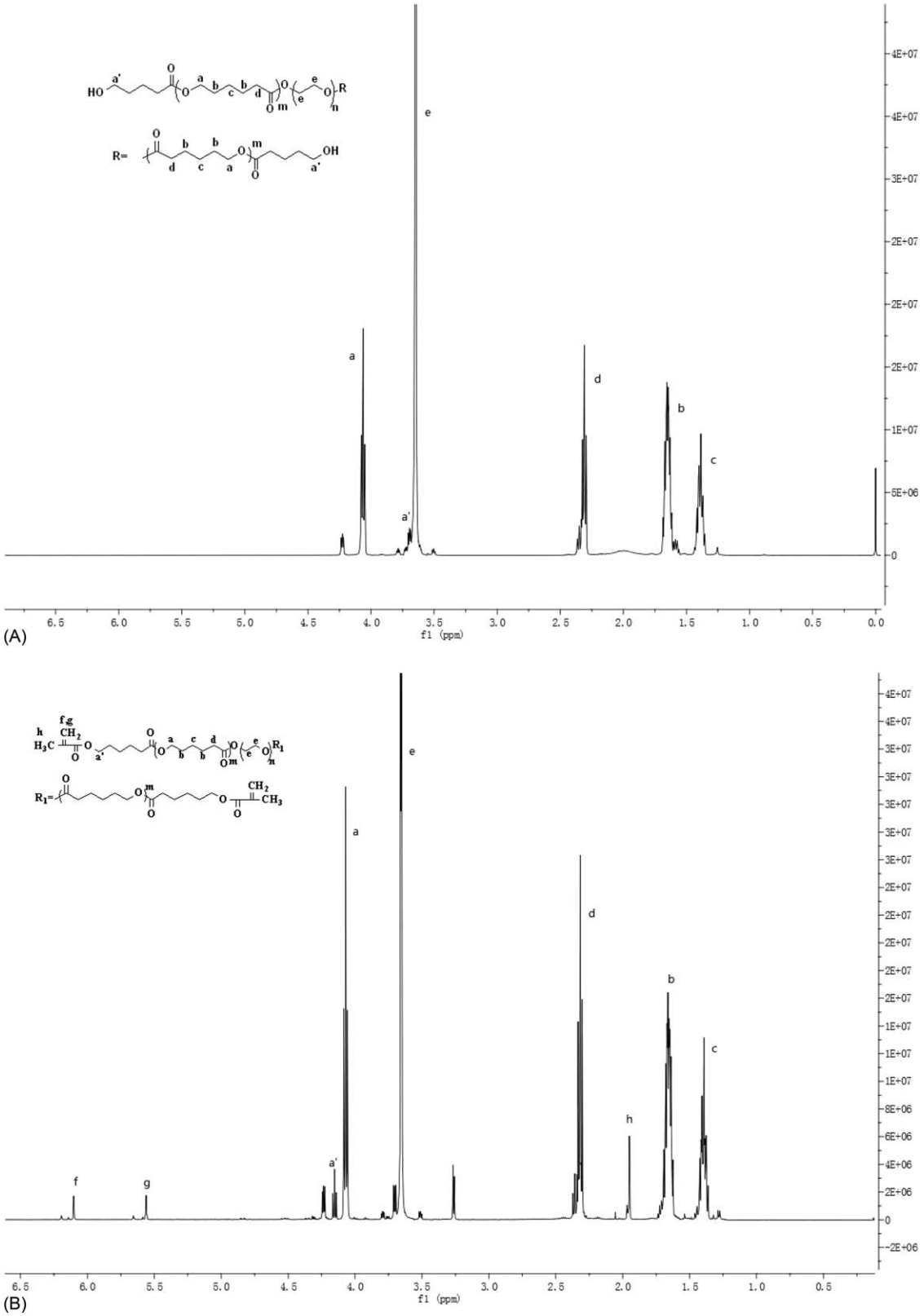

Figure 1. ^{1}H-NMR spectra of (A) CLPEGCL and (B) CLPEGCLMA.

shown in Figure 1(A), the characteristic peaks of the CLPEGCL segments were observed at 3.67 ppm ($HOCH_2$—, terminal methylene proton of PCL), 4.07 ppm [—(O)$COCH_2$—, methylene proton of PCL]; 2.32, 1.65, and 1.39 ppm (—CH_2—, methylene proton of PCL); and 3.66 ppm (—O—CH_2—CH_2—, the repeating unit of PEG). For the CLPEGCLMA [Figure 1(B)],

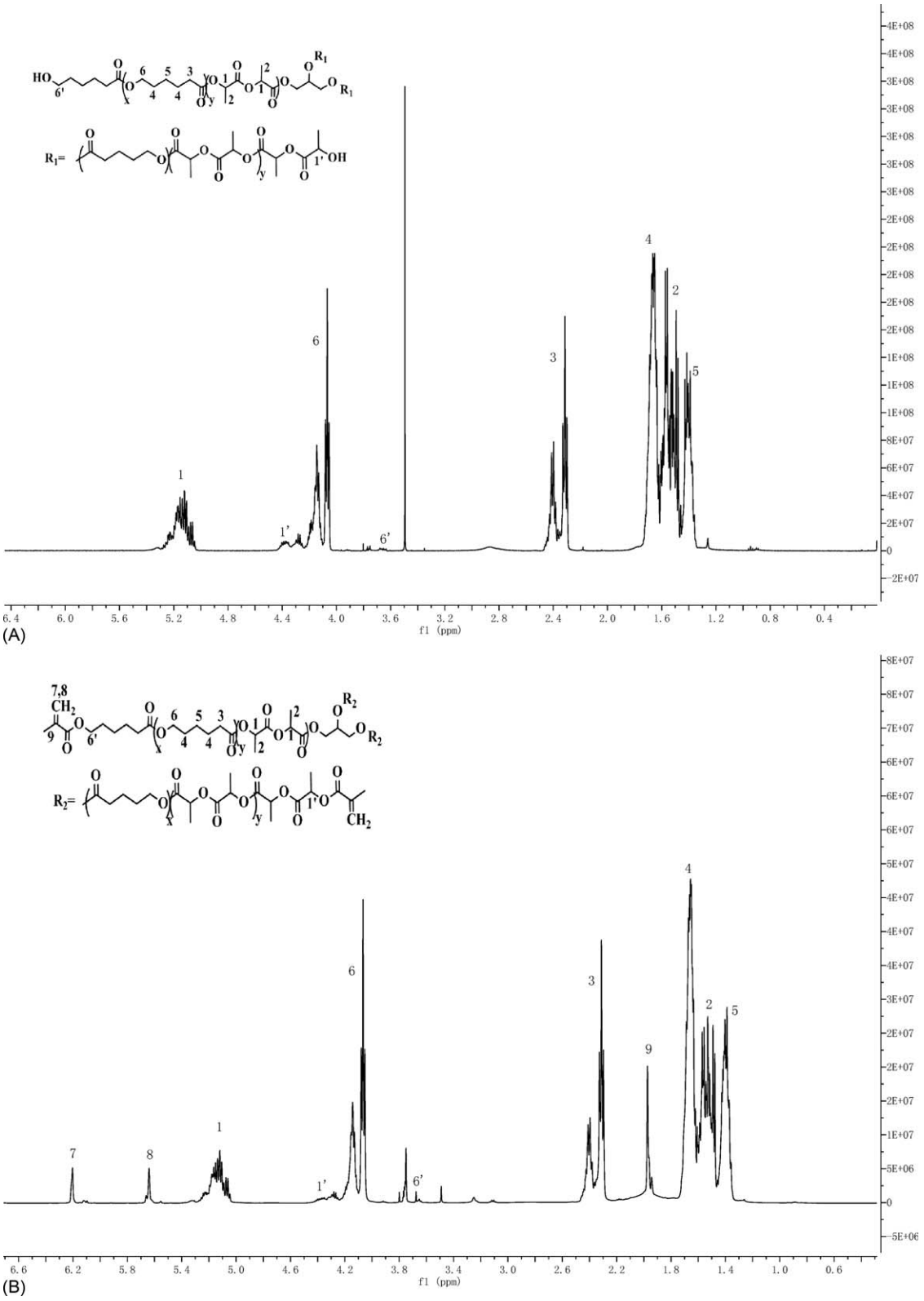

Figure 2. ^{1}H-NMR spectra of (A) SCP and (B) MASCP.

the signals at 5.56 and 6.10 ppm [CH_2═C(CH_3)─O─, vinyl protons] and 1.89 ppm [CH_2═C(CH_3)─O─, methyl protons] confirmed the presence of the methyl-acrylated group. DMA was assessed by a comparison of the values of the actual and theoretical ratios between the integrals of the methyl acrylate group (f + g) and the PEG unit (e) protons.

Table I. Compositions and Physical Data for the Synthesized Prepolymers

	M_n[a]	PDI[a]	Theoretical CL/LA ratio (mol/mol)	Actual CL/LA ratio (mol/mol)[b]	DMA (%)[c]
SCP-1	3960	1.34	12.5:7.5	13.7:6.3	—
MASCP-1	—	—	—	—	89.7
SCP-2	3432	1.32	10:10	10.8:9.2	—
MASCP-2	—	—	—	—	88.6
SCP-3	3655	1.36	7.5:12.5	6.7:13.3	—
MASCP-3	—	—	—	—	88.1
CLPEGCL	7551	1.08	—	—	—
CLPEGCLMA	—	—	—	—	87.6

[a] The M_n and PDI values of SCP and CLPEGCL were measured by GPC.
[b] The actual CL/LA ratio values were calculated on the basis of the ^{1}H-NMR data.
[c] The DMA values of MASCP and CLPEGCLMA were calculated on the basis of the ^{1}H-NMR data.

In Figure 2, the representative ^{1}H-NMR spectra of SCP and MASCP at a CL/LA ratio of 12.5:7.5 are illustrated. For the SCP [Figure 2(A)], distinct chemical shifts appeared at 5.04–5.27 and 4.34–4.45 ppm [—O—CH(CH_3)—C(O)—, methylidyne proton of PLA], 4.03–4.22 and 3.65–3.72 ppm (—OCH_2—, methylene proton of PCL), 2.38–2.47 ppm [—(O)$COCH_2$—, methylene proton of PCL], 1.63–1.73 and 1.36–1.41 ppm (—CH_2—, methylene proton of PCL), 1.46–1.51 ppm (—CH_3, methyl protons of PLA). The value of CL/LA was calculated from the ratio of the integral intensities between the methylene oxy protons of the PCL group and methylidyne proton of the PLA group $[(6 + 6')/(1 + 1')]$. Figure 2(B) shows the ^{1}H-NMR spectrum of MASCP. The peaks at 5.66 and 6.24 ppm (vinyl protons) and 1.96 ppm (methyl protons) were, respectively, attributed to the protons of the methyl acrylate group. DMA was determined by a comparison of the actual and theoretical ratios of the integrals of the methyl acrylate groups $(7 + 8)$ and lactyl units $(1 + 1')$.

The M_n and PDI values (measured via GPC) and the actual CL/LA ratio and DMA (calculated by ^{1}H-NMR analysis) are listed in Table I. Copolymer with M_n values ranging from 3432 to 7551 with a narrow distribution (PDIs = 1.08–1.36) were successfully synthesized. The DMA of methylacrylated prepolymers all exceeded 85%, and the actual CL/LA compositions of SCPs were very close to the theoretical values.

Elastomer Characterization

Typically, the porosity, degree of swelling, and crosslinking density of an elastomer as significant factors in biomaterial degradation and drug-releasing kinetics have been reported.[28,31] In this study, three elastomers containing different compositions of MASCP were prepared; these samples are abbreviated as x:y elastomer (where x:y indicates the CL/LA ratio). The physical and thermal properties of the elastomers are listed in Table II.

As shown in Table II, the GCs of the elastomers exceeded 89%; this indicated that a high crosslinking efficiency was achieved. The PV values decreased when the CL/LA ratio decreased, and the SD values were closely matched at about 50%. Additionally, the elastomers were rubbery at ambient temperature because of their low T_g values (−20.7 to −39.5°C). Moreover, the T_g increased as the CL/LA ratio decreased in accordance with Amsden's analysis, in which the crosslinking density was positively correlated with the variation of T_g.[28] Thus, this result may indicate that a higher crosslinking density was achieved in the elastomer as the CL/LA ratio decreased.

SEM Evaluation of the Elastomers

The results of the SEM examination of the morphology are given in Figure 3. The images show that both open and closed channels and internal cavities existed within the elastomers. The 12.5:7.5 elastomer and 10:10 elastomer [Figure 3(A–D)] exhibited nearly the same morphological features. However, as the CL/LA ratio decreased to 7.5:12.5 [Figure 3(E,F)], significant morphological changes with smoother sections and fewer cavities were observed.

In Vitro Degradation Study

To investigate the influence of the changes in the elastomer composition on the degradation, mass losses from the elastomers were monitored over a 25-week period in PBS. Furthermore, at each given time point, the pH of the medium was

Table II. Physical and Thermal Properties of the Elastomers

SCP M_n	CLPEGCL M_n	CLPEGCLMA (wt %)	Abbreviation	GC (%)	PV (mL/100 g)	SD (%)	T_g (°C)
3960	7551	30	12.5:7.5 Elastomer	90.6	39.8	48.9	−39.5
3432	7551	30	10:10 Elastomer	92.6	35.1	48.3	−25.6
3655	7551	30	7.5:12.5 Elastomer	89.7	34.4	50.6	−20.7

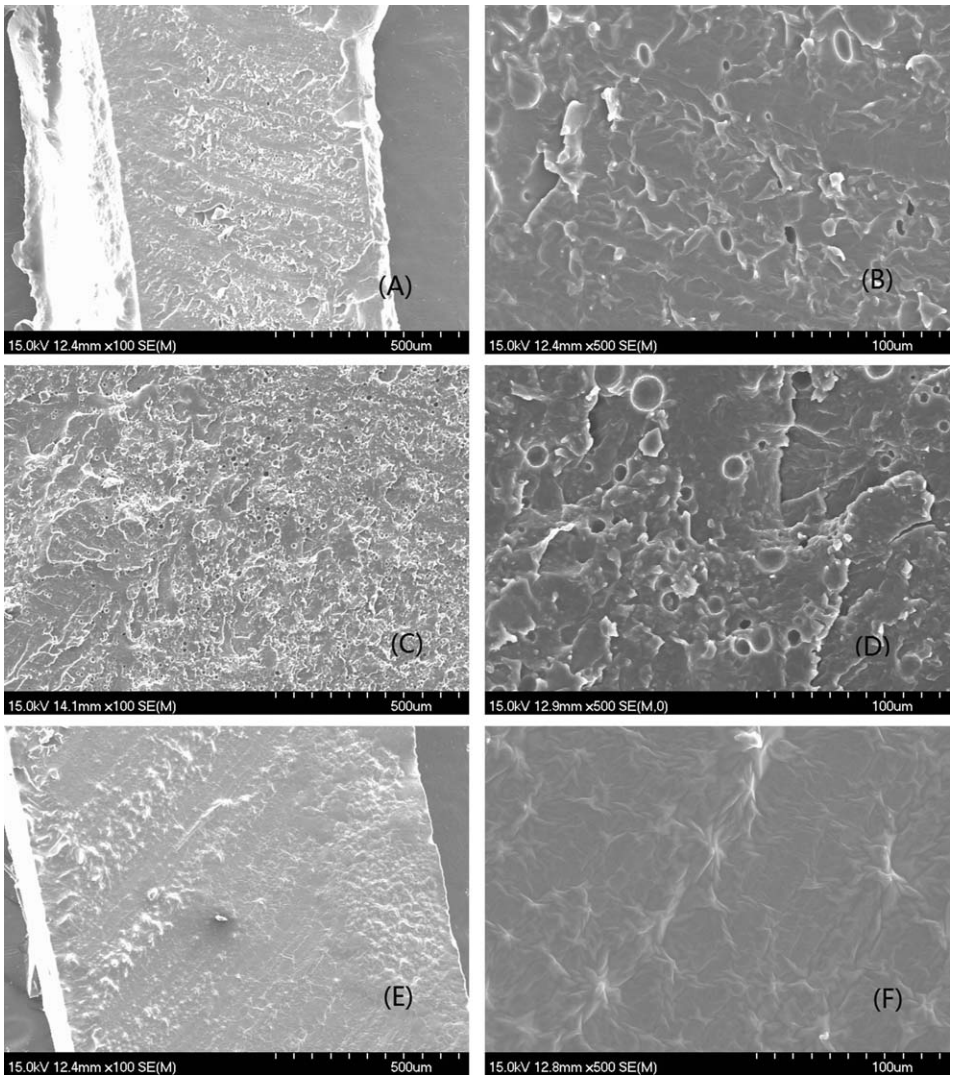

Figure 3. SEM images of the section morphologies: (A,B) 12.5:7.5 elastomer (100 and 500×), (C,D) 10:10 elastomer (100 and 500×), and (E,F) 7.5:12.5 elastomer (100 and 500×).

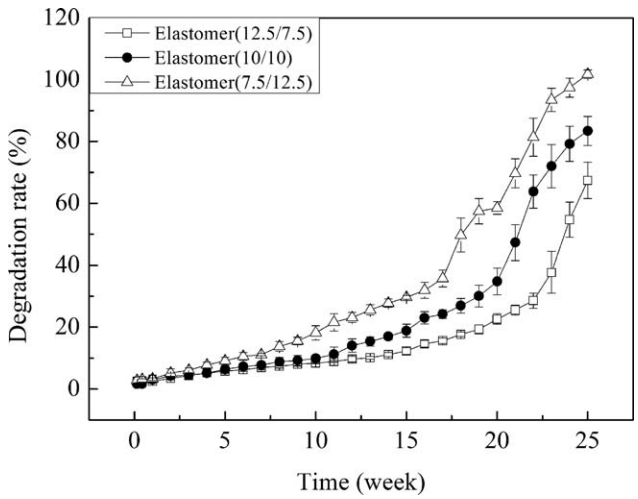

Figure 4. Degradation rates of the elastomers.

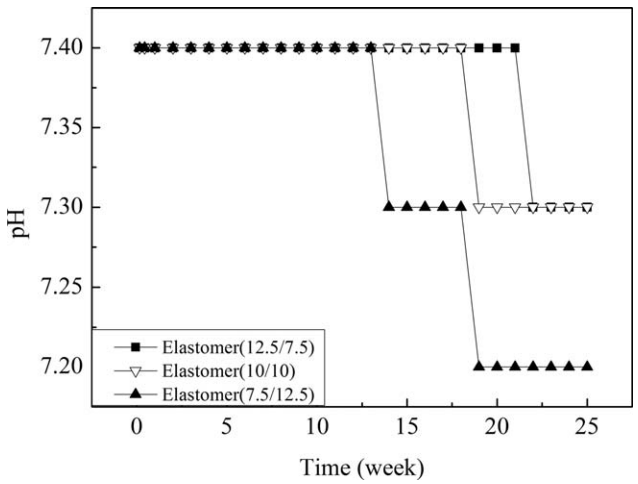

Figure 5. pH variations during degradation.

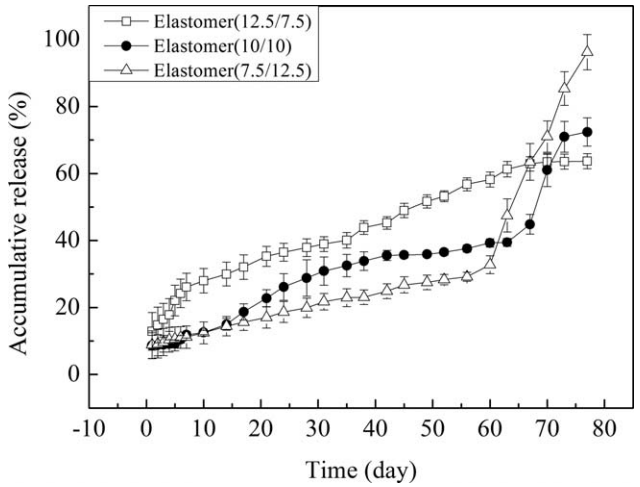

Figure 6. *In vitro* accumulative release of BSA.

measured. As shown in Figure 4, all of the elastomers displayed a three-phase degradation process; this could be characterized as follows: a slow, nearly constant degradation rate occurred in the first phase (0–7 weeks), and this was followed by a gradually accelerated process (8–17 weeks). The observable change in the dimensions of the prepared elastomers was not present until 17 weeks. At the end of the degradation period, the degradation rates for the 12.5:7.5 elastomer, 10:10 elastomer, and 7.5:12.5 elastomer reached 67.5, 83.5, and 100%, respectively. Figure 5 shows the variation of the pH values of the medium; this resulted from the hydrolysis of the ester bonds. As the CL/LA ratio decreased, the number of ester linkages increased, and more acidic oligomeric degradants were produced. Therefore, over time, the pH began to vary earlier, and accelerated degradation behavior (see Figure 4) was observed. In addition, in our previous studies on this system, the degradation conformed closely to the bulk degradation mechanism, and the SD and GC values were confirmed as the main influences on degradation. However, for the 12.5:7.5 elastomer, 10:10 elastomer, and 7.5:12.5 elastomer, the SD and GC values were only slightly changed. Obviously, in these elastomers, degradation was not only a function of the SD and GC but also a function of the accumulation of acidic oligomers in the medium. In all cases, these elastomers containing the new hydrophilic precursor blocks exhibited the majority of their mass losses (from 67.5 to 100%) in about 25 weeks. This degradation period was shorter than those observed for the previously reported lipophilic elastomers [based on acrylic tripoly(ε-caprolactone-*co*-D,L-lactide) cyclic esters[32] and trimethylene carbonate[33]].

In Vitro Release Study

The mechanisms of drug release from an elastomer can be complicated and variable. Most commonly, the process occurs via a diffusion-,[34] osmotic-pressure-,[35] or degradation-controlled[36] mechanism. In this study, the release kinetics of BSA from the elastomers over 77 days was evaluated, with the results shown in Figure 6. For the 12.5:7.5 elastomer, an initial fast release from 12.9 to 26.1% was observed during the initial 7 days, with a slow and nearly constant sustained release rate observed until the 70th day. Toward the end of the observation period, a

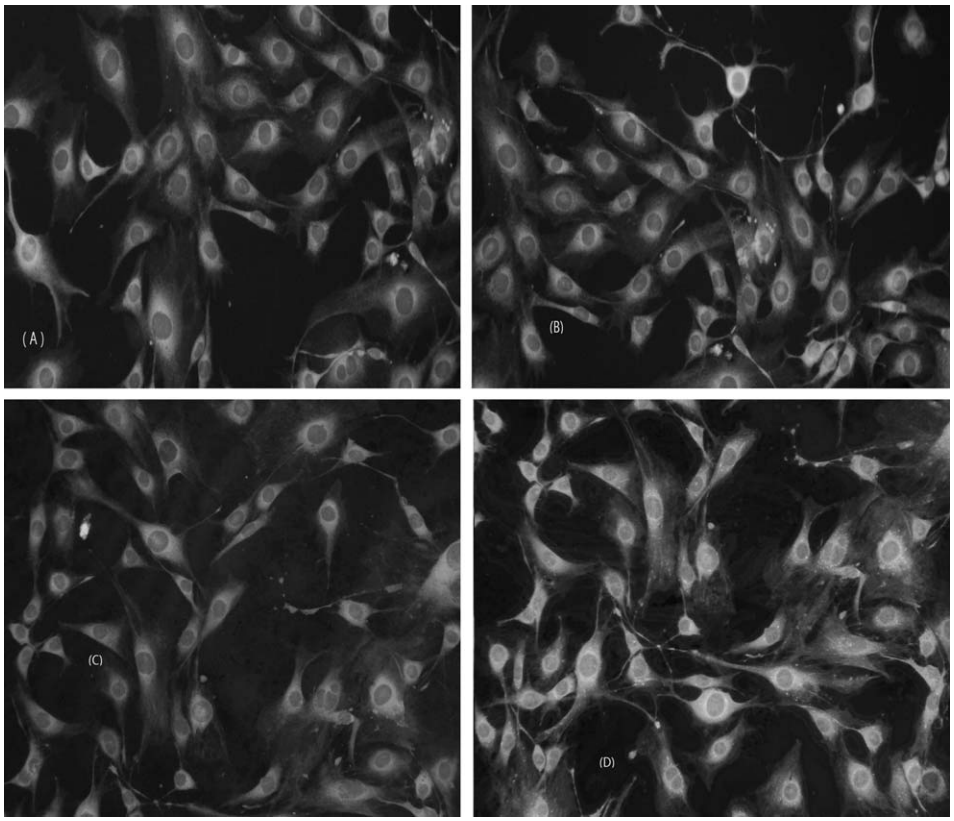

Figure 7. Morphology of the L929 fibroblast cells on the 7th day: (A) black, (B) 12.5:7.5 elastomer, (C) 10:10 elastomer, and (D) 7.5:12.5 elastomer.

Table III. Cytotoxicity Evaluation of the Elastomers over Different Incubation Times

	Cell viability (%)		
	2 days	4 days	7 days
12.5:7.5 Elastomer	98.86	96.81	93.71
10:10 Elastomer	98.71	93.78	91.05
7.5:12.5 Elastomer	95.30	92.49	89.89

nonrelease phase appeared. The total amount released was about 63.7%. For the 10:10 elastomer and 7.5:12.5 elastomer, the release curves were similar, and the process could be divided into two phases. Initially, a sustained and stable process with a low release rate was measured over the first 56 days. In this phase, the 10:10 elastomer exhibited a faster release rate than the 7.5:12.5 elastomer, and about 37.6 and 29.2% BSA, respectively, were released. In the second phase, a fast release process took place, and the total amounts of release were about 72.4 and 100%, respectively, after 77 days.

As indicated in Figure 6, over the first 60 days, BSA release occurred at a much faster rate than the degradation rate; therefore, the diffusion-controlled mechanism was considered the key mechanism for BSA release. This result was the same as that reported by Aryal *et al.*[9] During this period, the BSA-release rate increased as the CL/LA ratio increased. We speculated that the diffusion channel was more easily formed because of the larger PV values, weaker crosslinking densities (lower T_g values), and nearly constant SD values (cf. Table II). For the subsequent accelerated release process observed for the 10:10 elastomer and 7.5:12.5 elastomer, it was possible that most of the BSA was already released into the medium through diffusion channels, which were formed more quickly as time elapsed.

Cytotoxicity Assessment

The cytotoxicity and inflammatory effects of the elastomers were evaluated with the MTT assay and biological responses, respectively. For the cytotoxicity test, the L929 fibroblast cells were coincubated with the leaching solution of the elastomers

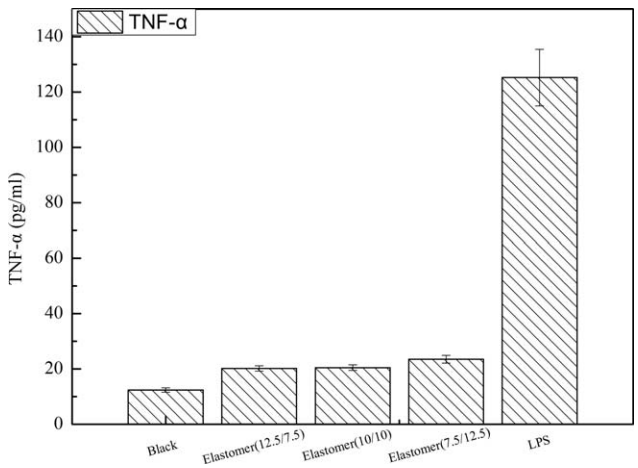

Figure 8. Concentration of TNF-α induced in each sterile degradation medium.

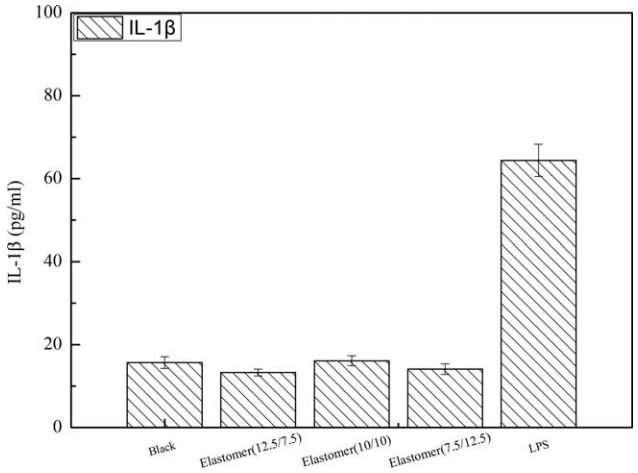

Figure 9. Concentration of IL-1β induced in each sterile degradation medium.

for 7 days. The morphologies of these cells on the 7th day are shown in Figure 7, and the results of the MTT viability assay are listed in Table III.

As shown in Figure 7, the L929 fibroblast cells did not exhibit significant morphological changes; this indicated that little harm was induced by the elastomer materials and the degradation products. From the MTT assay results, the values for cell viability for the different elastomers and various coincubation times were controlled within the range 89.89–98.86%. As the CL/LA ratio decreased or the coincubation times of the cells were extended, the cell viability appeared to decrease lightly. However, the high cell viability values indicated the safety of the elastomer materials. Additionally, RAW264.7 cells were used for biological response analysis. The concentrations of TNF-α and IL-1β induced in the cells were measured, and the results are shown in Figures 8 and 9, respectively. By comparing the positive and negative control media, we found that small amounts of TNF-α and IL-1β were generated; this suggested that the inflammatory effects were very slight. The results of the previous assays, therefore, confirm the good biocompatibility of these elastomers.

CONCLUSIONS

In summary, the preparation of elastomers consisting of MASCPs with various CL/LA compositions and CLPEGCLMA was demonstrated, and their physical and thermal properties were determined. The *in vitro* degradation study showed a nearly constant rate of degradation in the first 7 weeks; this was followed by a gradually accelerated process. The degradation rate could be altered by changes in the composition of CL/LA in the MASCP, and the accumulation of acidic degradation oligomers could accelerate the process of degradation. The BSA-release studies were performed for up to 77 days. Over the first 60 days, the BSA release from the elastomers was mainly controlled by a diffusion mechanism, and a sustained release process was evident. These results indicate that the variation in the structural design of the elastomer controlled its degradation and drug-release properties. Later, the changes in the release rate were mainly influenced by the breakdown of the elastomers.

Additionally, MTT analysis and inflammatory–induction experiments on the elastomers indicated good biocompatibility. Therefore, these elastomers may be attractive for applications in the controlled release of proteins.

ACKNOWLEDGMENTS

This study was financially supported by the National Natural Science Foundation of China (contract grant numbers 21376223 and 21106132).

REFERENCES

1. Albericio, F.; Kruger, H. G. *Fut. Med. Chem.* **2012**, *4*, 1527.
2. Topp, E. M. *AAPS J.* **2014**, *16*, 413.
3. Gupta, S.; Tyagi, R.; Parmar, V. S.; Sharma, S. K.; Haag, R. *Polymer* **2012**, *53*, 3053.
4. Agarwal, P.; Rupenthal, I. D. *Drug Discovery Today* **2013**, *18*, 337.
5. Liang, Y. Q.; Xiao, L.; Zhai, Y. L.; Xie, C. P.; Deng, L. D.; Dong, A. J. *J. Appl. Polym. Sci.* **2013**, *127*, 3948.
6. Bae, Y. H.; Huh, K. M.; Kim, Y.; Park, K. H. *J. Controlled Release* **2000**, *64*, 3.
7. Kenawy, E. R.; Bowlin, G. L.; Mansfield, K.; Layman, J.; Simpson, D. G.; Sanders, E. H.; Wnek, G. E. *J. Controlled Release* **2002**, *81*, 57.
8. Ahmed, T. A.; Ibrahim, H. M.; Samy, A. M.; Kaseem, A.; Nutan, M. T. H.; Hussain, M. D. *AAPS PharmSciTech* **2014**, *15*, 772.
9. Aryal, S.; Prabaharan, M.; Pilla, S.; Gong, S. Q. *Int. J. Biol. Macromol.* **2009**, *44*, 346.
10. Sohrabi, A.; Shaibani, P. M.; Etayash, H.; Kaur, K.; Thundat, T. *Polymer* **2013**, *54*, 2699.
11. Breitenbach, A.; Pistel, K. F.; Kissel, T. *Polymer* **2000**, *41*, 4781.
12. Yoon, H. Y.; Koo, H.; Choi, K. Y.; Kwon, I. C.; Choi, K.; Park, J. H.; Kim, K. *Biomaterials* **2013**, *34*, 5273.
13. Kamaly, N.; Xiao, Z. Y.; Valencia, P. M.; Radovic-Moreno, A. F.; Farokhzad, O. C. *Chem. Soc. Rev.* **2012**, *41*, 2971.
14. Ye, F.; Barrefelt, A.; Asem, H.; Abedi-Valugerdi, M.; El-Serafi, I.; Saghafian, M.; Abu-Salah, K.; Alrokayan, S.; Muhammed, M.; Hassan, M. *Biomaterials* **2014**, *35*, 3885.
15. Mukherjee, B.; Santra, K.; Pattnaik, G.; Ghosh, S. *Int. J. Nanomed.* **2008**, *3*, 487.
16. Park, W.; Kim, D.; Kang, H. C.; Bae, Y. H.; Na, K. *Biomaterials* **2012**, *33*, 8848.
17. Delgado-Rivera, R.; Rosario-Melendez, R.; Yu, W. L.; Uhrich, K. E. *J. Biomed. Mater. Res. A* **2014**, *102*, 2736.
18. Erdemli, O.; Usanmaz, A.; Keskin, D.; Tezcaner, A. *Colloids Surf. B* **2014**, *117*, 487.
19. Joo, K. I.; Xiao, L.; Liu, S. L.; Liu, Y. R.; Lee, C. L.; Conti, P. S.; Wong, M. K.; Li, Z. B.; Wang, P. *Biomaterials* **2013**, *34*, 3098.
20. Gaberc-Porekar, V.; Zore, I.; Podobnik, B.; Menart, V. *Curr. Opin. Drug Discovery Dev.* **2008**, *11*, 242.
21. Kolate, A. B. D.; Patil, S.; Vhora, I.; Kore, G.; Misra, A. *J. Controlled Release* **2014**, *192*, 67.
22. Yuan, W. Z.; Yuan, J. Y.; Zheng, S. X.; Hong, X. Y. *Polymer* **2007**, *48*, 2585.
23. Gu, F.; Neufeld, R.; Amsden, B. *J. Controlled Release* **2007**, *117*, 80.
24. Gu, F.; Younes, H. M.; El-Kadi, A. O. S.; Neufeld, R. J.; Amsden, B. G. *J. Controlled Release* **2005**, *102*, 607.
25. Chapanian, R.; Tse, M. Y.; Pang, S. C.; Amsden, B. G. *J. Pharm. Sci.* **2012**, *101*, 588.
26. Gu, F.; Neufeld, R.; Amsden, B. *Eur. J. Pharm. Biopharm.* **2007**, *66*, 21.
27. Sharifpoor, S.; Amsden, B. *Eur. J. Pharm. Biopharm.* **2007**, *65*, 336.
28. Amsden, B.; Qi, B. *Int. J. Pharm.* **2010**, *388*, 32.
29. Babasola, I. O.; Zhang, W.; Amsden, B. G. *Eur. J. Pharm. Biopharm.* **2013**, *85*, 765.
30. Shen, J.; Zhao, D. J.; Li, W.; Hu, Q. L.; Wang, Q. W.; Xu, F. J.; Tang, G. P. *Biomaterials* **2013**, *34*, 4520.
31. Kulkarni, A. R.; Soppimath, K. S.; Aminabhavi, T. M.; Rudzinski, W. E. *Eur. J. Pharm. Biopharm.* **2001**, *51*, 127.
32. Chapanian, R.; Tse, M. Y.; Pang, S. C.; Amsden, B. G. *J. Biomed. Mater. Res. A.* **2010**, *92*, 830.
33. Chapanian, R.; Tse, M. Y.; Pang, S. C.; Amsden, B. G. *Biomaterials* **2009**, *30*, 295.
34. Lemoine, D.; Francois, C.; Kedzierewicz, F.; Preat, W.; Hoffman, M.; Maincent, P. *Biomaterials* **1996**, *17*, 2191.
35. Shaker, M. A.; Younes, H. M. *Therapeut. Delivery* **2010**, *1*, 37.
36. Heller, J.; Barr, J. *Biomacromolecules* **2004**, *5*, 1625.